Distribution of Magnetic Moment in Hexagonal Cobalt*

R. M. Moon†
Lincoln Laboratory,‡ Massachusetts Institute of Technology, Lexington, Massachusetts
(Received 4 May 1964)

The magnetic form factor of hexagonal cobalt has been determined by measuring the coherent scattering of a polarized neutron beam from single-crystal samples. A Fourier inversion of the data indicates a nearly spherical distribution of positive moment around each atom, decreasing to a negative level in the space between atoms. A comparison of the results with calculated free-atom form factors shows that the observations can be accurately described by a model in which the net spin density is given by the sum of a positive free-atom $3d$ distribution and a negative constant. In terms of this model, the total moment per atom is composed of the following parts: $3d$ spin, $+1.86\pm0.07\ \mu_B$; $3d$ orbital, $+0.13\pm0.01\mu_B$; constant spin, $-0.28\pm0.07\mu_B$. The form factor showed no dependence on temperature between 78 and 300°K.

INTRODUCTION

THE periodic distribution of magnetic moment in a ferromagnet can be determined by precise measurements of the magnetic scattering amplitude in neutron diffraction experiments. A polarized neutron-beam technique[1] has recently been employed to investigate several metallic ferromagnets. Both the radial and angular dependence of the spin density have been determined for $Co_{0.92}Fe_{0.08}$,[2] Fe_3Al,[3] and Fe.[4] The present work extends these measurements to the case of hexagonal cobalt.

The measurements give the Fourier coefficients in the series expansion of the periodic magnetic-moment density; hence, density maps can be prepared from the data. Also, by comparing the data with calculated form factors, some idea of the identity of the electrons responsible for the magnetization may be obtained. Both of these approaches to the analysis of the data will be employed.

Knowledge of the spatial distribution of the $3d$ electrons is fundamental in understanding the properties of the transition metals. Magnetic form-factor measurements are one of the best methods of gaining such knowledge. However, the relationship between the observed magnetic-moment density and the $3d$ wave functions is not as direct as might be desired, and it is well to remember the following points when interpreting magnetic form factors of ferromagnetic metals. First, there is a small orbital contribution to the magnetization, and the measurements give the sum of the spin density plus the small orbital moment density. Second, the spin density itself is different from the charge density since spin-up electrons do not have the same radial density as spin-down electrons. This point has been emphasized in atomic calculations by Wood and Pratt[5] and Watson and Freeman.[6] Third, when the band structure of the transition metals is considered, the interpretation in terms of wave functions becomes even more complex. Wood[7] and Stern[8] have shown that in Fe a large difference between the radial wave functions at the top and bottom of the $3d$ band is to be expected. At the top of the band the wave functions are slightly contracted relative to the free-atom case, with small amplitude at half the nearest-neighbor distance. At the bottom of the band the wave functions are very diffuse with a large amplitude at half the nearest-neighbor distance. The observed spin density is associated with unpaired states near the top of the band plus a possible contribution from the "paired" electrons in the remainder of the band, as in the free-atom calculations of Watson and Freeman.[6] Fourth, there may be a contribution to the spin density from the conduction band and a very small contribution from the argon core. Despite these complications, magnetic form-factor measurements constitute one of the most direct methods of studying the distribution of $3d$ electrons in the transition metals.

EXPERIMENTAL TECHNIQUE

The experimental arrangement was identical to that described by Nathans *et al.*[1] The experiments were performed on two polarized neutron diffractometers installed at the MIT Nuclear Reactor. These instruments utilized the (200) reflection from a saturated $Co_{0.92}Fe_{0.08}$ crystal to produce the monochromatic polarized beam. The experiment consists of measuring the intensity in a Bragg peak when the incident neutrons are polarized antiparallel, and then parallel, to

---

* Based on a thesis submitted to the Department of Physics at the Massachusetts Institute of Technology, in partial fulfillment of the requirements for the degree of Doctor of Philosophy. This work was supported in part by the Lincoln Laboratory and in part by a grant from the National Science Foundation.

† Present address: Oak Ridge National Laboratory, Oak Ridge, Tennessee.

‡ Operated with support from the U. S. Air Force.

[1] R. Nathans, C. G. Shull, G. Shirane, and A. Andresen, Phys. Chem. Solids **10**, 138 (1959).

[2] R. Nathans and A. Paoletti, Phys. Rev. Letters **2**, 254 (1959).

[3] S. J. Pickart and R. Nathans, Phys. Rev. **123**, 1163 (1961).

[4] C. G. Shull and Y. Yamada, in *Proceedings of the International Conference on Magnetism and Crystallography, Kyoto, 1961* (Physical Society of Japan, 1962); C. G. Shull, in *Electronic Structure and Alloy Chemistry of the Transition Elements* (Interscience Publishers, Inc., New York, 1963), p. 69.

[5] J. H. Wood and G. W. Pratt, Jr., Phys. Rev. **107**, 995 (1957).

[6] R. E. Watson and A. J. Freeman, Phys. Rev. **120**, 1125, 1134 (1960).

[7] J. H. Wood, Phys. Rev. **117**, 714 (1960).

[8] F. Stern, Phys. Rev. **116**, 1399 (1959).

the sample magnetization. In an ideal experiment, the ratio of these two intensity measurements is given by

$$R=(1+\nu)^2/(1-\nu)^2, \quad (1)$$

where $\nu=p/b$, the ratio of the magnetic to nuclear scattering amplitudes. The magnetic scattering amplitude is related to the normalized form factor by

$$p(\mathbf{k})=(\gamma e^2/2mc^2)n_B f(\mathbf{k}), \quad (2)$$

where γ is the magnetic moment of the neutron in nuclear magnetons, n_B is the number of Bohr magnetons per atom in the sample, and $f(\mathbf{k})$ is the form factor. The assumption is made that the magnetic-moment distribution may be described in terms of a scalar density function, $\varrho(\mathbf{r})=\rho(\mathbf{r})\hat{K}$ where $\hat{K}$ is a unit vector in the direction of the bulk magnetization. In practice, Eq. (1) must be modified to take into account the operating characteristics of the instrument and various troublesome crystal effects. These corrections are briefly discussed in the following paragraphs: A more detailed discussion has been published elsewhere.[9]

Instrumental corrections. The data must be corrected for the effects of imperfect beam polarization, imperfect spin reversal, and $\frac{1}{2}\lambda$ contamination. Limits on the magnitude of these corrertions were obtained experimentally using an analyzing crystal ($\nu\approx 1$) in the test position. The uncertainty in these experimental corrections constituted the major source of error in the data for the inner reflections.

Secondary extinction. The secondary extinction effect was minimized by using thin crystals and small corrections were calculated to remove the residual effect. These calculations were based on experimental values of the mosaic width, determined by observing the shape of the crystal reflectivity curve in a double-crystal "parallel position" arrangement with a sharp Ge crystal in the monochromating position. The calculated extinction corrections were checked experimentally by varying the crystal thickness and neutron wavelength.

Simultaneous reflections. Closely allied to secondary extinction are the effects of simultaneous reflections.[10] When the crystal is oriented so that more than one Bragg reflection can occur, the intensity in any single reflected beam is modified by the presence of the other reflections. The crystal geometry was usually restricted to pillar shape to minimize the magnitude of this effect. In addition, the data were collected as the crystal was rotated in azimuth so that the presence of simultaneous reflections could be detected. Data showing a rapid variation with azimuth were not included in the average.

Magnetic anisotropy. One of the basic experimental requirements is that the sample be magnetized to saturation in the direction of the neutron polarization. It is difficult to satisfy this requirement in the case of hexagonal cobalt because of the high magnetic anisotropy. This difficulty was responsible for restricting the measurements to those reflections for which the deviation from the desired saturation was small. With the available field strength, saturation could be attained by magnetizing along the c axis or in the basal plane. Of the twenty reflections studied, ten experiments were performed with the applied field along the c axis and seven with the field in the basal plane. In all these cases, the beam depolarization was negligible as determined by polarization transmission experiments. In two of the remaining three cases, the measured polarization transmission was combined with a calculation of the angle between the applied field and the magnetization, based on the known anisotropy constants, to give a small correction to the data. The remaining reflection showed zero magnetic scattering and all corrections were unnecessary.

Sample purity and preparation. A supply of high-purity cobalt was obtained through the courtesy of F. R. Morral of the Cobalt Information Center, Battelle Memorial Institute. This material was in the form of polycrystalline cylinders of 99.95% purity.[11] Two single crystals were prepared from this material. Small corrections were applied to the data to remove the effect of the major impurities, Ni and Fe. Samples were cut either in the shape of pillars (approximately $0.1\times0.2\times1.0$ cm) or disks (approximately 1.0 cm in diameter). The samples were polished on fine (000) emery paper to reduce the beam depolarization at the surface.[9]

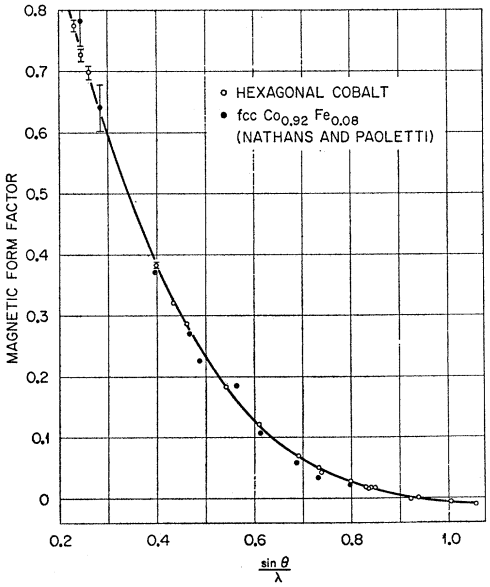

FIG. 1. The magnetic form factor of hexagonal cobalt compared with the fcc case. The solid line was drawn to emphasize the smooth decrease in the hexagonal form factor, indicating almost spherical symmetry.

[9] R. M. Moon, MIT Lincoln Laboratory Technical Report No. 312, 1963 (unpublished).

[10] R. M. Moon and C. G. Shull, Acta Cryst. **17**, 805 (1964).

[11] F. R. Morral, J. Metals **10**, 662 (1958).

Stacking faults. It is well known that hexagonal cobalt crystals have a strong tendency toward faulting. These faults may be described as an interruption in the normal hexagonal layer stacking sequence along the c axis by the inclusion of a local fcc stacking sequence. The local environment of an atom is such a faulted region would appear more nearly cubic than hexagonal. Since the form factors for the two structures differ very little, as shown in Fig. 1, we expect a negligible influence on the hexagonal form factor due to faulting. Although no experiments were performed to measure the form factors in crystals which were known to have different degrees of faulting, it is believed that the general reproducibility of the results for different crystals lends support to the above argument.

Temperature effects. Implicit in the interpretation of the data is the assumption that the outer electrons follow the nuclei in their thermal motion; hence the Debye-Waller factors for nuclear and magnetic scattering are equal. Menzinger and Paoletti[12] have observed that there is a change in the polarized neutron results for fcc cobalt when the temperature is changed from 300–873°K. This is taken to be an indication that either the spin distribution is temperature-dependent or that the nuclear and magnetic Debye-Waller factors are not equal. In the present investigation a comparison of results on three reflections, the (100), (200), and (300), was made at room temperature and 77°K. No significant difference was observed in the effective form factor at these two temperatures. To interpret their results, Menzinger and Paoletti suggest that the mean-square electronic displacement may be smaller than the mean-square nuclear displacement, $\langle u_e^2\rangle_{\rm av}=0.37\langle u_n^2\rangle_{\rm av}$. The present results indicate that $\langle u_e^2\rangle_{\rm av}=(1\pm0.15)\langle u_n^2\rangle_{\rm av}$ over the temperature range from 77–300°K. The two results are not necessarily inconsistent. A more general relationship may exist, $\langle u_e^2\rangle_{\rm av}=G(T)\langle u_n^2\rangle_{\rm av}$, where $G(T)$ equals unity at low temperatures and decreases as the temperature increases. An alternate explanation of the results of Menzinger and Paoletti has been advocated by Weiss.[13] He assumes that the spin-up and spin-down charge densities change with temperature in such a way that their sum is constant and their difference gives the Menzinger and Paoletti result. In any event, the position taken here is that at room temperature the nuclear and electronic Debye-Waller factors are equal, and that the form factor does not change between 300 and 77°K.

RESULTS

To determine the absolute value of the magnetic scattering amplitudes, it is necessary to know the nuclear coherent scattering amplitude. Two independent determinations of the nuclear amplitude were obtained by measuring neutron-diffraction powder patterns for pure cobalt metal and Co_3O_4. The average value for the two experiments was $b=0.250\pm0.003\times10^{-12}$ cm, in good agreement with the results of Roth.[14] The quoted error in the value of b was based on counting statistics and internal consistency of the two experiments. In both experiments there were possible sources of systematic error which were difficult to evaluate, but which might increase the error in b to $\pm0.01\times10^{-12}$ cm. In calculating the magnetic scattering amplitudes from the measured values of p/b, a 1% error in b has been assumed. In a later section we will return to this question, to see whether a larger error in b would have any important consequences.

The results of the polarized beam experiments are summarized in Table I. Using the above value for b, the normalized form factor values were obtained from Eq. (2) with $n_B=1.707$.[15] The values of $\sin\theta/\lambda$ were calculated using $a=2.5059$ and $c=4.0695$, as determined by Morral.[11]

In Fig. 1 the hexagonal form factor is compared with the results of Nathans and Paoletti[2] on fcc $Co_{0.92}Fe_{0.08}$. There is a small but significant difference in the two sets of data in the high $\sin\theta/\lambda$ region. It is uncertain to what extent the iron, which is present in the cubic case, is responsible for this difference. The aspherical effects, indicated by departure from a smooth function, are more pronounced in the cubic case, and this could be responsible for some difference in the two sets of data. The radial spin density must be similar in the two cases.

One important conclusion can be reached immediately by inspection of Fig. 1. The smooth decrease of the experimental points in the hexagonal case indicates that the magnetic moment distribution must be almost spherical.

The rather large number of reflections in the hexa-

TABLE I. The magnetic form factor of hexagonal cobalt.

hkl	$\sin\theta/\lambda$	p/b	f
010	0.2304	1.424 ±0.010	0.774 ±0.010
002	0.2457	1.335 ±0.014	0.726 ±0.010
011	0.2611	1.283 ±0.014	0.697 ±0.011
110	0.3991	0.704 ±0.005	0.383 ±0.005
013	0.4347	0.591 ±0.005	0.321 ±0.004
020	0.4608	0.527 ±0.003	0.286 ±0.004
014	0.5428	0.334 ±0.002	0.182 ±0.002
120	0.6096	0.223 ±0.002	0.121 ±0.002
030	0.6912	0.1297±0.0014	0.0705±0.0011
032	0.7336	0.0926±0.0007	0.0503±0.0006
006	0.7372	0.0794±0.0010	0.0432±0.0006
220	0.7982	0.0519±0.0015	0.0282±0.0008
130	0.8307	0.0351±0.0014	0.0191±0.0008
222	0.8351	0.0302±0.0009	0.0164±0.0005
116	0.8383	0.0306±0.0008	0.0166±0.0005
034	0.8481	+0.0297±0.0010	+0.0161±0.0006
040	0.9216	−0.0030±0.0022	−0.0016±0.0012
224	0.9374	+0.0002±0.0015	+0.0001±0.0008
230	1.0043	−0.0110±0.0020	−0.0060±0.0011
140	1.0559	−0.0194±0.0014	−0.0105±0.0008

[12] F. Menzinger and A. Paoletti, Phys. Rev. Letters **10**, 290 (1963).
[13] R. J. Weiss, Phys. Rev. Letters **11**, 264 (1963).
[14] W. L. Roth, Bull. Am. Phys. Soc. **8**, 213 (1963).
[15] H. P. Myers and W. Sucksmith, Proc. Roy. Soc. (London) **A207**, 427 (1951).

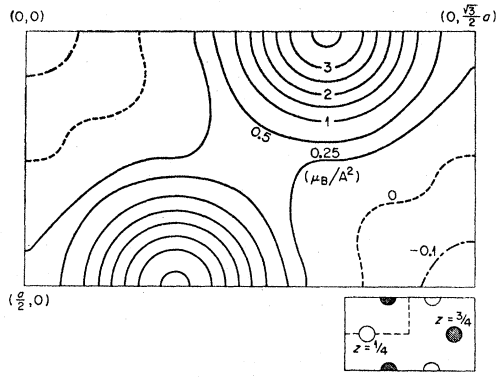

FIG. 2. Projection of magnetic moment density on basal plane. Lower right diagram shows projected position of atoms in orthorhombic unit cell. Dashed lines indicate portion of cell shown in density map.

gonal case and the difficulties associated with the magnetic anisotropy precluded the collection of sufficient data for an accurate three-dimensional inversion. However, all reflections of type $(hk0)$ were measured out to $\sin\theta/\lambda=1.06$. These data have been used to make a Fourier projection of the distribution onto the basal plane, using the 7090 computer at the MIT Computation Center.

The projected density is given by

$$\rho=n_B A^{-1}\sum_h\sum_k F_{hk0}\exp(-i\mathbf{k}_{hk0}\cdot\mathbf{r}), \qquad (3)$$

where n_B is the number of Bohr magnetons per atom, A is the area of the unit cell projection and

$$F_{hk0}=\sum_j f_{hk0}\exp(i\mathbf{k}_{hk0}\cdot\mathbf{r}_j), \qquad (4)$$

where the summation goes over the atomic positions within the unit cell. For this inversion, the hexagonal structure was represented in terms of an orthorhombic cell of dimensions $(a, \sqrt{3}a, c)$ with atoms at $(0, \frac{1}{3}, \frac{3}{4})$, $(0, \frac{2}{3}, \frac{1}{4})$, $(\frac{1}{2}, \frac{1}{6}, \frac{1}{4})$, $(\frac{1}{2}, \frac{5}{6}, \frac{3}{4})$. The results are shown in Fig. 2. The spherical nature of the distribution is apparent from the fact that the first six contour lines shown around each site are actually circles within the arithmetic round-off error of the computer program. In interpreting the outer contour lines, it must be remembered that the two atoms are on different levels, resulting in the apparent overlap of the distributions. The true nearest-neighbor distance is greater than the projected distance by a factor of $\sqrt{3}$. Of particular interest is the negative moment in the regions farthest from any atom. The plot indicates that a nearly constant negative plateau of projected density is reached at sufficient distance from the atoms. The suggested picture is that of almost spherical mountains of positive moment localized around each atom and partially immersed in a sea of negative moment.

This negative density is more apparent in Fig. 3, which is a plot of the profile of the projected density along a line parallel to the [100] vector in the hexagonal reciprocal lattice. In this figure, point C is the center of a structural hole. It corresponds to position C in the familiar ABC stacking nomenclature, and is empty in the hexagonal structure. If the region between atoms is filled with a nearly uniform negative spin density, then the best value for the magnitude of this density is to be found at point C in the projection. Also shown in Fig. 3 is a resolution function obtained by including the same number of terms in the series but using a constant form factor for each reflection. The resolution function shows the diffraction effects which would be obtained in attempting to map a lattice of point atoms with data from the same set of reflections used in the cobalt projection. Any detail in the cobalt spin density on a scale smaller than the width of the central maximum of the resolution function cannot be resolved. In examining Figs. 2 and 3 one should not forget the effects of finite resolution and the fact that these figures represent the integrated magnetic-moment density along the direction of the c axis over a distance $z=c$. For both of these reasons one should not expect to see the decrease in $3d$ spin density near the nuclear sites.

It is believed that the regions of negative density do not result from experimental errors in the magnetic amplitudes nor from the series termination error. One indication of the importance of the series termination error is in the size of the density oscillations in the cobalt projection of Fig. 3. Any diffraction rings which are present are on a smaller scale than the indicated

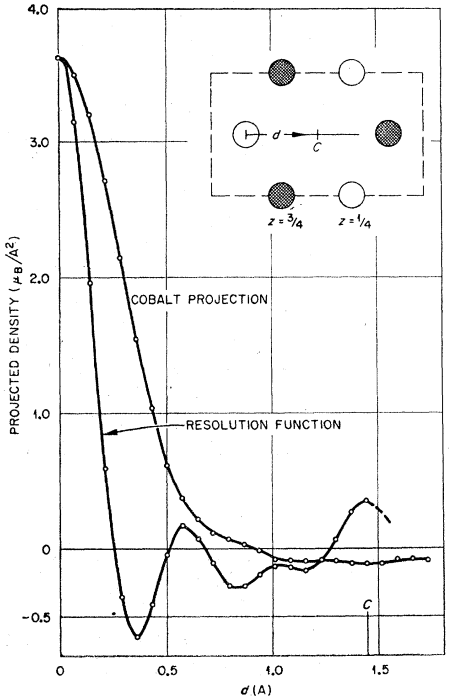

FIG. 3. Profile of projected density along the indicated line. The resolution function has been normalized to equal the cobalt projection at $d=0$.

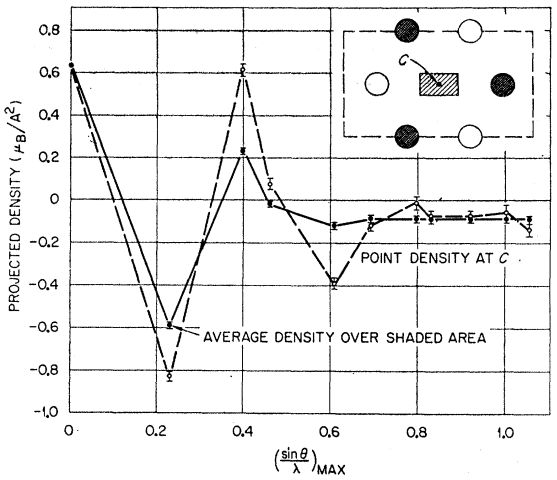

FIG. 4. Conversion of Fourier series for projected density at point C and for average projected density over area around point C, of size $0.2a\times0.2\sqrt{3}a(\delta=0.1)$. Successive points were calculated by increasing the number of terms in the series by one

negative level. A more convincing case can be made by studying the effect of changing the number of terms included in the series. The projected density at point C is given by

$$\rho_C=n_BA^{-1}\sum_h\sum_k F_{hk0}\,, \tag{5}$$

where F_{hk0} are the orthorhombic structure factors. Let us also ask for the average density over a rectangle centered on point C of size $(2\delta a\times2\sqrt{3}\delta a)$. It is easily shown that this average density is given by

$$\bar{\rho}_C(\delta)=n_BA^{-1}(2\pi\delta)^{-2}\times\sum_h\sum_k (hk)^{-1}F_{hk0}\sin(2\pi h\delta)\sin(2\pi k\delta)\,. \tag{6}$$

The factor $(hk)^{-1}$ makes the convergence of the series for the average density much faster than that for the point density series.[16]

In calculating the average density we are asking a less detailed question than in the point density case, and can get an accurate answer with less input data. The values of ρ_C and $\bar{\rho}_C$, with $\delta=0.1$, are shown in Fig. 4 as a function of the maximum value of $\sin\theta/\lambda$. The indicated errors are based on the experimental errors given in Table I. At high values of $(\sin\theta/\lambda)_{\max}$, the point density still shows oscillations of appreciable magnitude, but $\bar{\rho}_C$ has converged very nicely. If we take the amplitude of the oscillations as an indication of the series termination error, then for ρ_C the error is about $0.04\ \mu_B/A^2$, and for $\bar{\rho}_C$ the error is about $0.002\ \mu_B/A^2$. In the latter case the series-termination error is insignificant compared to the experimental error in the density. Even in the point-density case, the series definitely appears to be approaching a negative limit.

[16] The author is indebted to W. Marshall for suggesting this approach to the series termination problem.

The limiting value for $\bar{\rho}_C$ of $-0.085\ \mu_B/A^2$ corresponds to an average magnetic field of -2.4 kg. This is the average field in a pillar containing the center of the unit cell, of dimensions $0.2a\times0.2\sqrt{3}a\times c$.

What is the origin of this negative magnetic-moment density? It is tempting to assign it to negative-spin polarization in the conduction band. However, this conclusion cannot be justified without prior knowledge of the spin distribution in the $3d$ band. Unfortunately, we have only free-atom calculations available with which to make a quantitative comparison.

FORM-FACTOR ANALYSIS

In comparing experimental and free-atom form factors, we are testing a model in which a periodic density function is constructed by superposition of atomic functions centered at each atomic site,

$$\rho'(\mathbf{r})=\textstyle\sum_i \rho_a(\mathbf{r}-\mathbf{r}_i)\,. \tag{7}$$

Here, ρ_a is a normalized free-atom density function, with form factor

$$f(\mathbf{k})=\int\rho_a(\mathbf{r})e^{i\mathbf{k}\cdot\mathbf{r}}dv\,. \tag{8}$$

The form factor, $f'(\mathbf{k})$, for the periodic function, $\rho'(\mathbf{r})$, is nonzero only when $\mathbf{k}$ satisfies the Bragg condition. For this set of scattering vectors, $\mathbf{k}_{hkl}$, the crystal form factor is equal to the free-atom form factor, $f_{hkl}'=f(\mathbf{k}_{hkl})$.

In constructing the free-atom form factor, contributions to the magnetic moment density from the following sources were considered: spin polarization of the outer electrons, orbital moment of the unquenched $3d$ electrons, and spin polarization of the argon core. Each of these sources may be further divided into spherical and aspherical parts. We neglect all the aspherical contributions except that arising from the $3d$ spin. The total form factor is written as

$$f=\frac{2}{g}f_s^s+\frac{g-2}{g}f_0^s+f_c^s+\frac{2}{g}f_s^a\,, \tag{9}$$

where the subscripts s, 0, and c refer to spin, orbital and core, and the superscripts s and a refer to spherical and aspherical. The g factor determines the fraction of the total moment due to spin polarization and the fraction due to unquenched orbital motion. Its value for metallic cobalt is 2.17, based on the magnetomechanical experiments of Scott.[17]

In the case of Fe, Shull and Yamada[4] found that the experimental results were in good agreement with a combination of free-atom $3d$ and $4s$ form factors. It was necessary to assume that the $4s$ polarization was opposite in direction to the $3d$ polarization. We have seen

[17] G. G. Scott, in *Proceedings of the International Conference on Magnetism and Crystallography, Kyoto, 1961* (Physical Society of Japan, 1962).

that the Fourier inversion of the cobalt data also shows the presence of a diffuse negative polarization. Let us therefore build a constant negative-spin polarization into our model and at the same time increase the $3d$ spin contribution to maintain the normalization. The form factor for a constant density is $\delta(\mathbf{k})$, so we rewrite Eq. (9) as

$$f=\frac{2}{g}[(1+\alpha)f_{s3d}{}^{s}-\alpha\delta(k)] + \frac{g-2}{g}f_0{}^{s}+f_c{}^{s}+\frac{2}{g}(1+\alpha)f_{s3d}{}^{a}. \quad (10)$$

Equation (10) describes the model we wish to test against the experimental data. While the introduction of the δ function may seem arbitrary, it is really quite natural. The Fourier analysis of any periodic function in a specified lattice can be resolved into three questions concerning the shape, scale and average value of the function. The periodic function can be written as

$$\rho(\mathbf{r})=A_0+\sum_j A_j \exp(-i\mathbf{k}_j\cdot\mathbf{r}), \quad (11)$$

where the index j runs over all the allowed Bragg reflections except the (000). The shape of the function is determined by the relative size of the A_j, the scale is determined by the absolute values of the A_j, and the average value is determined by A_0. Two functions, ρ^a and ρ^b have the same shape if $A_j{}^a=KA_j{}^b$, where K is a constant defining the relative scale of the two functions. In the present analysis, we wish to ask whether the shape of the observed periodic spin density is the same as that produced by superimposing atomic $3d$ spin densities according to Eq. (7). The proper way to ask this question is to test for proportionality between the observed and calculated form factors for all reflections other than (000). From this point of view, the introduction of the δ function is merely a convenient way to separate the questions of shape and scale from that of the average value. Practically speaking, this treatment is equivalent to that of Shull and Yamada, because their $4s$ atomic form factor almost goes to zero before the first Bragg reflection.

Aspherical Form Factor

Let us first examine the experimental data to see if there is any evidence that the term in $f_s{}^a$ is nonzero. The outer portion of the experimental form factor is shown on a greatly enlarged scale in Fig. 5. The only striking departure from a smooth curve is the (006) point, and the pair of points near $f=0$ seem out of line. The data shown in Fig. 5 have been analyzed in terms of crystalline-field effects, following the treatment of Weiss and Freeman.[18] In the hexagonal case, the

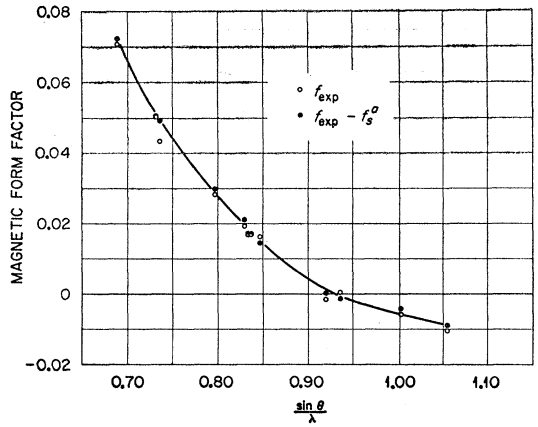

FIG. 5. Effect of aspherical spin distribution on high-angle results. Solid points should fall on a smooth curve.

crystalline field splits the $3d$ electrons into three substates, two doubly degenerate levels with rotational properties like xy, x^2-y^2 and yz, xz and a single level like $3z^2-r^2$. The total aspherical form factor is written as a linear combination of the aspherical form factors for the three substates,

$$f_{s3d}{}^a=(0.4+\epsilon)f^a(E_{2g})+(0.4+\eta)f^a(E_{1g}) + (0.2-\epsilon-\eta)f^a(A_{1g}). \quad (12)$$

The parameters ϵ and η measure the departure from spherical symmetry. When $\epsilon=\eta=0$, the three terms on the right of Eq. (12) add to zero. The work of Weiss and Freeman[18] and Watson and Freeman[19] allow the calculation of the f^a for each substate, based on free-atom wave functions. It was possible to obtain values of ϵ and η from the experimental data without using any calculated spherical form factors. Details of this analysis are given in Appendix A. The best values are $\epsilon=-0.006$ and $\eta=0.016$. An experimental spherical form factor was then obtained by subtracting the small aspherical contribution from the experimental data. This spherical form factor is shown in Fig. 5 as the solid circles. If the analysis is valid, these points should lie on a smooth curve. This analysis gives a reasonably consistent interpretation in terms of crystal-field effects, but the very small departure from spherical symmetry implies a small crystalline-field splitting in comparison to the $3d$ bandwidth.

It is worth noting that the calculated form factors are quite sensitive to changes in the population; that is, the form factors for the substates are widely different. For example, for the (006) reflection $f^a(E_{2g})=+0.238$, $f^a(E_{1g})=-0.255$, and $f^a(A_{1g})=+0.034$; while the observed $f_s{}^a$ is only -0.006.

The implications of this analysis may be better visualized with the help of Fig. 6. The whole analysis

[18] R. J. Weiss and A. J. Freeman, Phys. Chem. Solids **10**, 147 (1959).

[19] R. E. Watson and A. J. Freeman, Acta Cryst. **14**, 27, 231 (1961).

is based on the assumption that the wave function can be separated into a radial and an angular part. Shown in Fig. 6 is the θ dependence of the square of the angular part of the wave function for each substate and for the sum of the three substates, weighted by the indicated population. The largest effect is in the c direction where the distribution deviates from the spherical case by about 6%.

Radial Form Factor

The contribution of the core polarization term of Eq. (10) was estimated from unpublished calculations of Watson and Freeman for iron. It is quite small, the largest contribution for any of the reflections being only 0.003.

Three different calculations by Freeman and Watson were considered in estimating the spherical part of the spin and orbital contributions of the $3d$ electrons. Two of these were restricted Hartree-Fock calculations for an outer electron configuration of $3d^74s^2$ and $3d^84s^1$. The other was a spin polarized Hartree-Fock calculation for a $3d^74s^2$ configuration. The spin form factors for the two restricted calculations have been published,[19] and the remainder of the calculated results were privately communicated. By subtracting the orbital, core, and aspherical contributions from the experimental form factor, and then testing the resulting experimental spin form factor for proportionality with the calculated spin form factors, it was possible to judge whether the calculated-$3d$ spin density had the same shape as the observed density distribution. It was quickly apparent

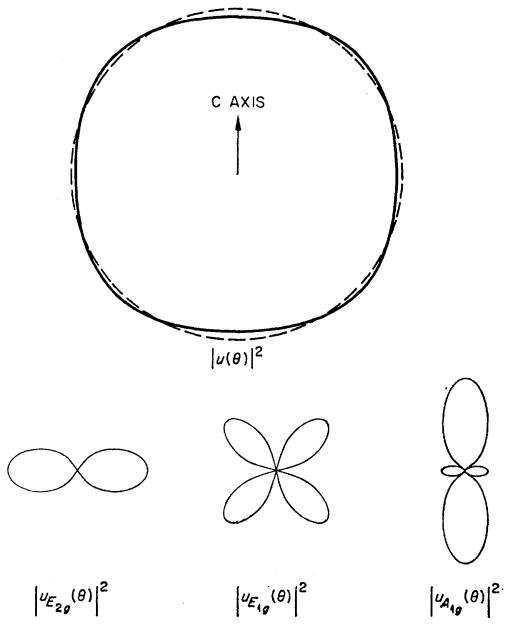

FIG. 6. Angular dependence of the spin density in hexagonal cobalt. Dashed circle is for spherical symmetry, solid figure is for $|u(\theta)|^2=0.394|u(E_{2g})|^2+0.416|u(E_{1g})|^2+0.190|u(A_{1g})|^2$.

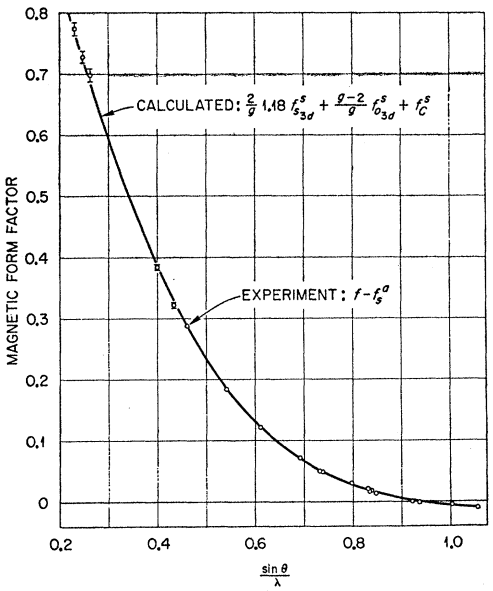

FIG. 7. Comparison of experimental results for hexagonal cobalt with free-atom calculation when $\alpha=0.18$. The free-atom form factor is based on a $3d^74s^2$ spin-polarized Hartree-Fock calculation by Watson and Freeman.

that the spin-polarized $3d^74s^2$ calculation is the best, and it is very good indeed. The comparison between the calculated and experimental form factors is illustrated in Fig. 7. The points are the experimental values minus the small aspherical contribution and the solid line is given by the first four terms of Eq. (10) with $\alpha=0.18$.

The remarkable agreement illustrated in Fig. 7 shows that the shape of the periodic spin distribution is accurately given by the proposed model. Let us return to the question of the effect of uncertainty in the nuclear scattering amplitude. The conclusion about the shape of the distribution is independent of the nuclear amplitude, because this conclusion rests only on the relative sizes of the f_{hkl}. A large error in b will only introduce an uncertainty in the proportionality factor $(1+\alpha)$. The most pessimistic view of the error in b is 4%, whereas b would need to be 18% lower to avoid introducing the negative spin density. In terms of our model, and assigning a 4% error in $(1+\alpha)$, the net magnetic moment per atom is distributed as follows:

$3d$ spin	$+1.86\pm0.07\ \mu_B$,
constant spin	$-0.28\pm0.07\ \mu_B$,
$3d$ orbital	$+0.13\pm0.01\ \mu_B$.

It is interesting to compare the value of the constant polarization introduced in the form-factor analysis with the level of the negative density seen in the Fourier inversion. A constant spin density of $-0.28\ \mu_B$/atom corresponds to a projected density onto the basal plane of $-0.10\ \mu_B/A^2$, in good agreement with the level indicated in Fig. 3.

SUMMARY AND DISCUSSION

The Fourier inversion has shown that the magnetic moment in cobalt looks like an almost spherical distribution of positive moment localized around each atomic site, decreasing to a negative level in the region between atoms. The purpose of the form-factor analysis was to see if this distribution could be described in terms of some more familiar atomic distribution. It was found that the spin distribution can be accurately represented as the sum of two parts; one looks like a superposition of calculated atomic-3*d*-density functions located at each atomic site and the other is a negative constant. One should be cautious in ascribing significance to the form-factor analysis beyond the fact that it is a convenient way to describe the observed spin distribution. In particular, we cannot claim that this analysis proves the existence of a constant negative polarization in the conduction band or that the spin density in the 3*d* band is just like that calculated for the free atom. All that can be said with certainty is that the sum of the polarization in the 3*d* and conduction bands has the spatial dependence described by the model.

The appearance of a contribution to the spin polarization which is similar in shape to the calculated free-atom distribution is not surprising. On the basis of the band theory calculations[7,8] for Fe, the unpaired spin distribution, which is derived from a group of states near the top of the band, is expected to be similar to the calculated free-atom distribution. The diffuse negative polarization is more difficult to understand, although the theoretical approach of Anderson[20] seems promising. The contribution of the paired electrons near the bottom of the 3*d* band should also be considered in relation to the diffuse negative spin density. The unrestricted Hartree-Fock calculations for free atoms[5,6] show that the paired 3*d* electrons produce a negative spin density at large radii. The combination of this effect and the diffuse wave functions near the bottom of the 3*d* band might help in understanding these results.

ACKNOWLEDGMENTS

It is a pleasure to acknowledge the help and advice of Professor C. G. Shull in all phases of this research. The author has profited through stimulating discussions with J. B. Goodenough and A. J. Freeman. F. R. Morral, A. Wold, and R. Nathans have been generous in supplying the cobalt of various forms used in this work. N. Menyuk and K. Dwight made valuable contributions in the powder measurements on Co_3O_4. The following members of the MIT Neutron Diffraction Group gave valuable assistance: W. C. Phillips, D. O. Murray, G. Stucky, S. Spooner, and A. D'Addario.

APPENDIX: ASYMMETRY ANALYSIS

The separation of the experimental form factor into spherical and aspherical parts is not quite so straightforward as in the cubic case, where there are a number of different pairs of reflections occurring at the same value of $\sin\theta/\lambda$. Such pairs occur in the hexagonal case only if the structure is perfectly close packed. Since cobalt is almost a perfect close-packed structure, there are pairs of reflections at almost the same value of $\sin\theta/\lambda$. Substituting (12) into (10) and grouping the spherical parts in a single term, the total form factor is

$$f=f^s+\epsilon'[f^a(E_{2g})-f^a(A_{1g})]+\eta'[f^a(E_{1g})-f^a(A_{1g})], \quad \text{(A1)}$$

where $\epsilon'=(2/g)(1+\alpha)\epsilon$ and $\eta'=(2/g)(1+\alpha)\eta$. The difference between the form factors for a pair of reflections at nearly the same value of $\sin\theta/\lambda$ is

$$\Delta f=\frac{df^s}{d(\sin\theta/\lambda)}\Delta\left(\frac{\sin\theta}{\lambda}\right)+\epsilon'\Delta[f^a(E_{2g})-f^a(A_{1g})]+\eta'\Delta[f^a(E_{1g})-f^a(A_{1g})]. \quad \text{(A2)}$$

Because the experimental data showed such a small aspherical contribution, the slope of the spherical part could be accurately estimated from the data by drawing a smooth curve through the points. In the above equation, Δf is the observed form-factor difference between two reflections, the first term on the right was estimated from the data, and the form factors in the last two terms were calculated as outlined below. Thus, each such pair of reflections gives a linear equation in ϵ' and η'. Seven pairs of reflections in the high-angle region were considered and the best values of ϵ' and η' were selected to satisfy all seven equations simultaneously. For the selected values of ϵ' and η', the calculated and observed values of Δf were in reasonable agreement in six of the seven cases.

Based on the work of Weiss and Freeman,[18] the following expressions for the coefficients of ϵ' and η' were obtained:

$$f^a(E_{2g})-f^a(A_{1g})=-\frac{10}{7}(1-3\cos^2\beta)\langle j_2\rangle-\frac{15}{56}(3-30\cos^2\beta+35\cos^4\beta)\langle j_4\rangle, \quad \text{(A3)}$$

$$f^a(E_{1g})-f^a(A_{1g})=-\frac{5}{14}(1-3\cos^2\beta)\langle j_2\rangle-\frac{15}{28}(3-30\cos^2\beta+35\cos^4\beta)\langle j_4\rangle. \quad \text{(A4)}$$

β, the angle between the normal to the reflecting planes and the c axis, is determined by

$$\cos^2\beta=\frac{l^2}{\frac{4}{3}(c/a)^2(h^2+hk+k^2)+l^2}. \quad \text{(A5)}$$

The functions $\langle j_2\rangle$ and $\langle j_4\rangle$ were taken from the work of Watson and Freeman,[19] based on a restricted Hartree-Fock calculation for a $3d^7$ configuration.

[20] P. W. Anderson, Phys. Rev. 124, 41 (1961).